

Cavity Dynamics behind a 2-D Wedge Analyzed by Incompressible and Compressible Flow Solvers

Sunho Park¹, Heebum Lee², Hak-Kyu Choi², Shin Hyung Rhee², Yohan Choe³, Hyeongjun Kim³, Chongam Kim³, Ji-Hye Kim⁴, Byoung-Kwon Ahn⁴, Hyoung-Tae Kim⁴

¹ Dept. Ocean Engineering, Korea Maritime and Ocean Univ., Busan, Korea

² Dept. Naval Architecture and Ocean Engineering, Seoul National Univ., Seoul, Korea

³ Dept. Aerospace Engineering, Seoul National Univ., Seoul, Korea

⁴ Dept. Naval Architecture and Ocean Engineering, Chungnam National Univ., Daejeon, Korea

E-mail: shr@snu.ac.kr

Abstract. To study the cavity dynamics behind a two-dimensional wedge, a pressure-based numerical solver for incompressible cavitating flow and a density-based numerical solver for compressible cavitating flow solvers were developed, respectively, using a cell-centered finite volume method. Cavity interface was captured based on an approximation of homogeneous mixture flow. Cavity dynamics analysed by the two developed solvers were compared and validated against experimental data. Cavity shape and length, re-entrant jet, and vortical cavity shedding were compared and discussed.

1. Introduction

Cavitation is often observed in high-speed hydrodynamic mechanical devices. Cavitation is usually treated an undesirable phenomenon, however, it is regarded as desirable phenomenon for military purposes, e.g., torpedoes. Controlled super-cavitation was used for torpedoes to reduce the skin-friction drag. To make use of super-cavitation, understanding its physics and predicting its behaviour are essential.

Many studies concerning super-cavitation have been done for decades. Ahn et al. [1] experimentally studied cavity dynamics behind the 2D wedge. Park et al. [2] developed incompressible cavitating flow solver and simulated cavitation around a 2D wedge and the wedge with a body, respectively.

The objectives of the present study were (1) to develop a pressure-based incompressible cavitating flow solver and a density-based compressible cavitating flow solver, (2) to understand the compressibility and thermodynamic effects on cavity dynamics behind a 2D wedge using the two developed solvers.

2. Problem Description

The 2-D wedge geometry for the present study is shown in Figure 1. The wedge shape was defined by angle (α), chord (c), and depth (d). The wedge angle of 15 degrees, chord length of 75.96 mm, and depth of 20 mm were selected for the present study. The Reynolds number (Re) was based on the free-stream velocity (U_∞) and the wedge depth (d). The cavitation number (σ) was defined as (P_σ -



$P_v)/0.5\rho U_\infty^2$, where P_v was the vapour pressure, P_o was the reference pressure and ρ was the fluid density. The cavitation number was in the range of 0.08 to 2.34. Cavitation begins to form in the low-pressure region behind the wedge as in the backward facing step flow and propagates downstream as shown in Figure 1.

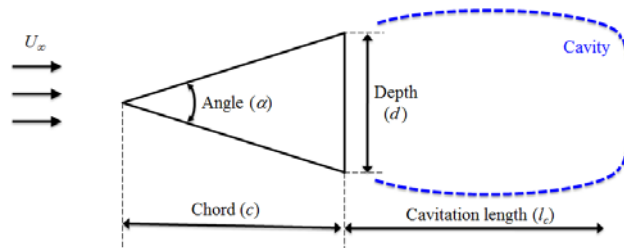


Figure 1. Problem description of wedge.

3. Computational Methods

3.1. Incompressible cavitating flow solver

The governing equations consist of mass- and momentum conservation equations for the mixture fluid with a volume fraction transport equation formulated by pressure-based methods. A preconditioning is applied in the pressure correction step to cover the whole Mach-number region [2].

3.2. Compressible cavitating flow solver

Assuming fully compressible flows including thermodynamic effects, the governing equations consist of mixture mass-, momentum-, and energy-conservation equations, together with a one-phase mass-conservation equation formulated by density-based methods. A preconditioning is introduced to cover the low-Mach-number region.

4. Model Tests

The experimental observations were carried out in the cavitation tunnel at Chungnam National University. The tunnel's test section has a cross section of 100 mm wide, and 100 mm high. The maximum speed of the tunnel free stream was 20 m/s and the pressure was controlled from 10 to 300 kPa. The cavity length and dynamics were observed for various wedge shapes. Figure 2 is a snapshot of the cavity behind the wedge for cavitation numbers of 0.35 and 0.40 with the Reynolds number of 1.7×10^5 . The observed cavity lengths (l_c/d) were 5.45 and 3.84 for cavitation numbers of 0.35 and 0.40, respectively.

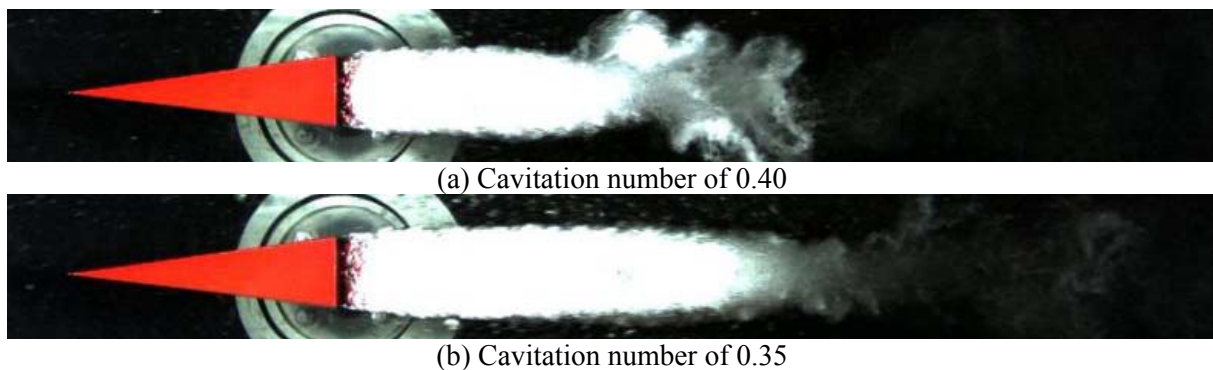


Figure 2. Snap shot of cavity behind the wedge in experiment

5. Results and Discussion

Figure 3 shows the volume fraction contours and streamlines around the 2D wedge. The cavitating flow shows recirculation behind the wedge, which was separated from the outer flow. Re-entrant jet was not observed in the incompressible flow, while it was clearly shown in the compressible flow. The streamlines were similar in both cases.

Figure 4 shows the contours of non-dimensionalized streamwise velocity component around the wedge. The circulating flow produced by the incompressible flow solver was stronger than that by the compressible flow solver. It was evident by the stronger negative streamwise velocity component, i.e., toward the upstream, at $y=0$ in the incompressible flow solution.

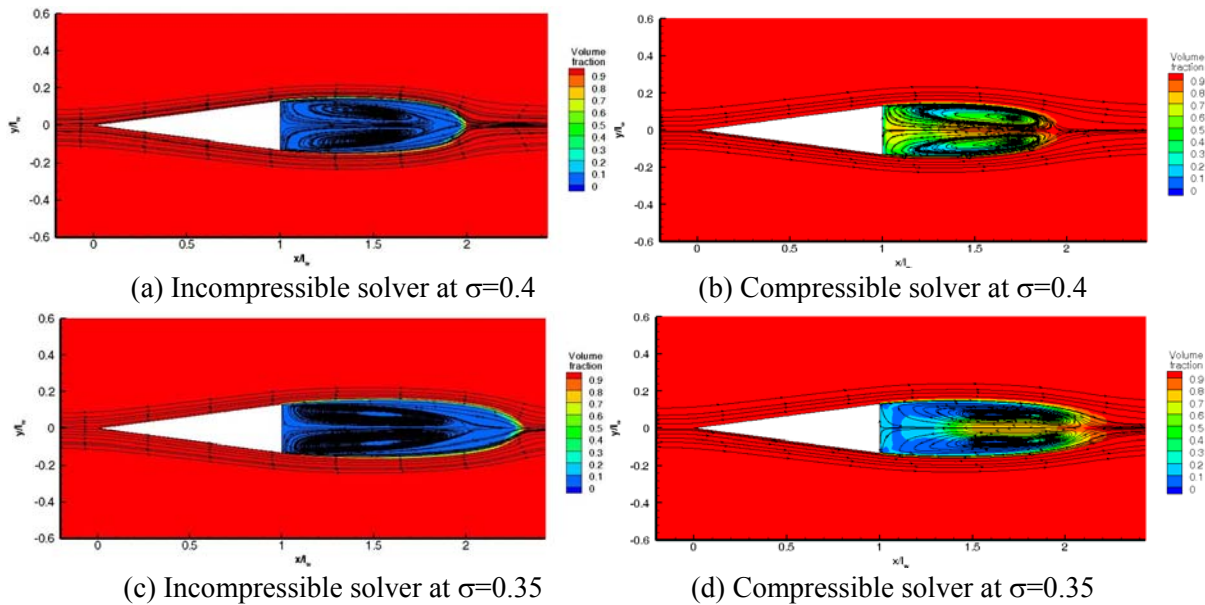


Figure 3. Volume fraction contours and streamlines around wedge

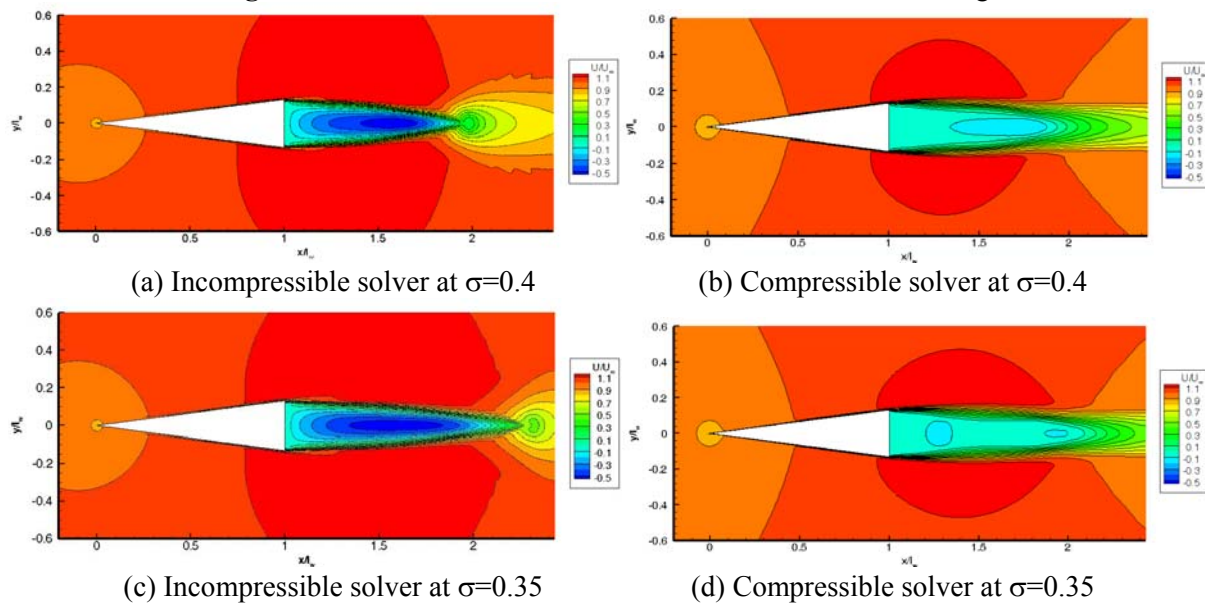


Figure 4. Nondimensionalized streamwise velocity component contours around wedge

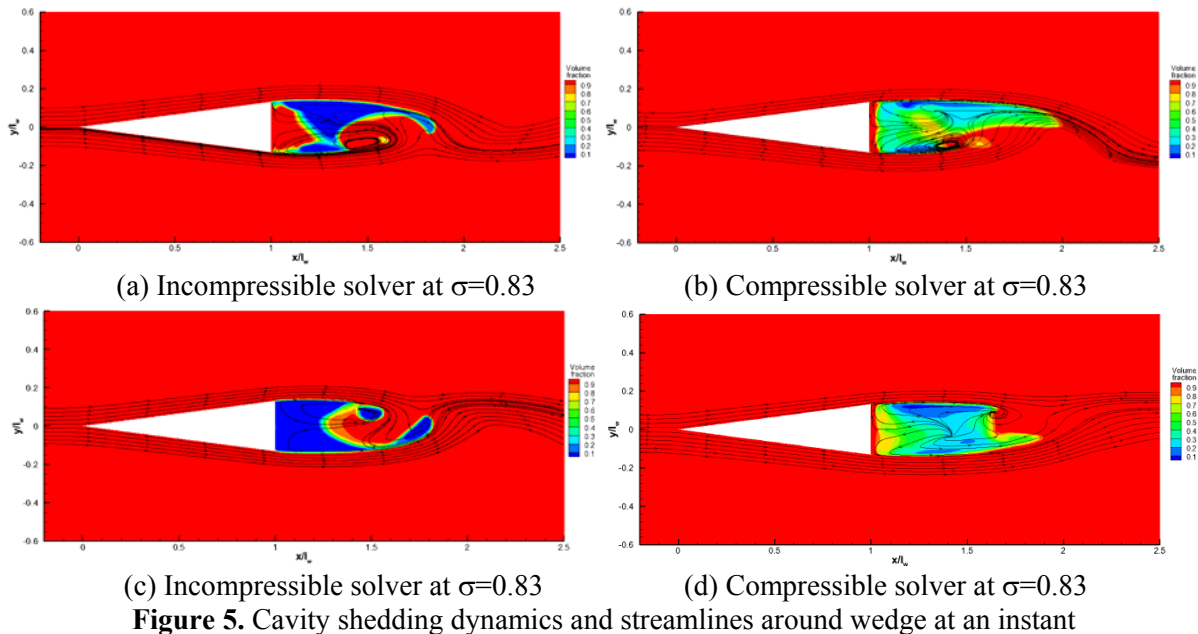
The computed cavity lengths are compared with experimental results and analytic solution [1, 2], listed in Table 1. Cavity lengths were calculated using a vapour volume fraction value of 0.5. The cavity length grew longer as the cavitation number decreased. The cavity lengths predicted by the two

solvers were somewhere between the experimental data and analytic solution. The cavity lengths computed by the incompressible flow solver were longer than that by the compressible flow solver. This tendency was prominent at low cavitation number. Re-entrant jet observed in the compressible flow solver was believed to be the cause of shorter cavity length.

Table 1. Cavity length.

$\pi\sigma/2d$	Incompressible flow	Compressible flow	Experiment	Analytic solution
2.1	5.07	4.73	5.45	4.42
2.4	3.83	3.65	3.84	3.56

Cavity shedding was observed with cavitation number of 0.83 and the Reynolds number of 1.7×10^5 . On issues such as the cavity shedding, the shedding is related to the Reynolds number and the cavity is related to cavitation number. Figure 5 shows the volume fraction contours and streamlines at an instant. The cavity shedding was different for both solvers. The compressibility and thermodynamic effects influenced cavity shedding dynamics.



6. Concluding Remarks

The cavity lengths, velocity and pressure contours around a 2D wedge were studied by a pressure-based incompressible cavitating flow solver and a density-based compressible cavitating flow solver, respectively. The circulation strength and re-entrant jet were different for both solvers. The cavity shedding dynamics was weakened by the compressibility and thermodynamic effects in the compressible flow solver.

7. References

- [1] Ahn B K, Lee C S and Kim H T 2010 Experimental and numerical studies on supercavitating flow of axisymmetric cavitators *Int J Naval Archit Ocean Eng* **2** 39–44
- [2] Park S and Rhee S H 2012 Computational analysis of turbulent super-cavitating flow around a two-dimensional wedge-shaped cavitator geometry *Computers & Fluids* **70** 73-85